Influence of the successive annealing on the magnetization processes in Fe_73.5Cu_1Nb_3Si_15.5B_7 ribbon

Sabolek, Stjepan; Marohnić, Željko; Herzer, Giselher

Source / Izvornik: **Fizika A, 1996, 5, 185 - 196**

Journal article, Published version
Rad u časopisu, Objavljena verzija rada (izdavačev PDF)

Permanent link / Trajna poveznica: https://urn.nsk.hr/urn:nbn:hr:217:058896

Rights / Prava: In copyright / Zaštićeno autorskim pravom.

Download date / Datum preuzimanja: **2024-03-29**

Repository / Repozitorij:

Repository of the Faculty of Science - University of Zagreb

ISSN 1330–0008
CODEN FIZAE4

INFLUENCE OF THE SUCCESSIVE ANNEALING ON THE MAGNETIZATION PROCESSES IN $Fe_{73.5}Cu_1Nb_3Si_{15.5}B_7$ RIBBON

STJEPAN SABOLEK, ŽELJKO MAROHNIĆ[a] and GISELHER HERZER[b]

Department of Physics, Faculty of Science, University of Zagreb, POB 162, Zagreb, Croatia
[a] *Institute of Physics of the University, University of Zagreb, POB 304, Zagreb, Croatia*
[b] *Vacuumschmelze GmbH, D-63450 Hanau, Germany*

Received 21 November 1996

UDC 538.955

PACS 75.50.Kj, 75.60.-d, 75.60.Ch

The model for the influence of core–current generated field H_p on the magnetization processes in ferromagnetic ribbons has been employed for the detailed analysis of the $M-H$ loops and the corresponding $\mathrm{d}M/\mathrm{d}t$ vs. H curves for $Fe_{73.5}Cu_1Nb_3Si_{15.5}B_7$ alloy, successively annealed at different temperatures $T_a \leq 540$ °C. The analysis shows that in the amorphous state ($T_a \leq 300$ °C), only fraction of the main (inner) domain structure participates in the process of magnetization. Further annealing strongly reduces the local anisotropy and the average pinning strength of the domain walls $< S_u >$, which results in a very low coercive field H_c for 400 °C $\leq T_a \leq$ 500 °C. Simultaneously, the maximum magnetization M_m becomes almost equal to the saturation magnetization M_s (≈ 1.3 T) already in low magnetizing field ($H_0 = 100$ A/m). The minimum of H_c ($T_a = 450$ °C) is associated with the formation of nanocrystalline Fe_3Si grains, and high M_m and maximum permeability μ_{max} and a low angle $< \delta >$ (between domain magnetizations and the ribbon axis) show that a whole domain structure is very simple in this range of T_a. Further annealing ($T_a > 500$ °C) increases $< S_u >$ and $< \delta >$ (which increases H_c) and reduces drastically μ_{max} which is consistent with the earlier results for similar samples.

1. Introduction

Recent investigations have shown that ferromagnetic materials consisting of two different phases, i.e. fine structure of nanocrystalline grains dispersed within the amorphous matrix, may possess exceptionally good soft ferromagnetic properties [1]. Such structures can be obtained by annealing of the amorphous Fe-Cu-Nb-Si-B alloys at suitable temperature [2,3]. In particular, for the $Fe_{73.5}Cu_1Nb_3Si_{13.5}B_9$ alloy, the best properties (very low coercive field H_c and high initial permeability μ_i) are obtained for the annealing at temperatures T_a between 500 °C and 550 °C [2,3]. The improvement of the soft magnetic properties is caused by the formation of the fine structure of Fe_3Si nanocrystalline grains (with randomly oriented easy axes of magnetization), dispersed within the amorphous matrix which presents the coupling for the interaction between these grains [2,3]. The magnetocrystalline anisotropy energy K of Fe_3Si compound is very large ($K \approx 10^4$ J/m^3), however, when the grain diameter D is smaller than the exchange length l_k, the magnetizations of the particular grains can not follow the direction of the easy axes of the grains because of the exchange interaction between the grains. Therefore, the effective magnetic anisotropy within the sample tends to vanish, which results in extremely soft magnetic properties [2,3].

The investigation of the domain structure and the magnetization processes is particularly important for further improvement of the soft magnetic properties of these materials. Earlier studies have shown that the application of the model for the influence of surface fields H_p (generated with the direct (J_D) or alternating (J) core current) on the process of magnetization of amorphous ferromagnetic ribbons [4–7] may provide a good insight into the domain structure, anisotropy and pinning of domain walls (DW) in such samples [8,9]. In particular, the analysis of the influence of H_p on the $M-H$ loops and the $\mathrm{d}M/\mathrm{d}t$ vs. H curves allows to estimate the average angle $< \delta >$ between the magnetizations (I) of the individual groups of domains (which contribute to magnetization of the sample) and the ribbon axis, and of the average pinning strength $< S_u >$ of the corresponding DWs [8]. It is particularly important that in this simple manner one can gain an insight into the main (inner) domain structure (MDS) and the relevant magnetization mechanisms. Such investigations of the $Fe_{73.5}Cu_1Nb_3Si_{15.5}B_7$ ribbon (hereafter FeCuNbSiB) in the amorphous state [10] have shown that its very bad soft magnetic properties (high H_c, low maximum magnetization M_m, all in relatively low magnetizing fields, $H_0 \leq 300$ A/m) are associated with very strong local anisotropy which is probably due to internal stresses, structural defects and inhomogeneities in these samples [11].

Here we use the analysis of the $M-H$ loops (obtained with and without core currents J and J_D) for the discussion of the changes in the domain structure, DW pinning and the magnetization mechanisms of FeCuNbSiB sample during the successive annealing at different temperatures T_a. We also consider some possibilities for the further decrease of H_c and loss E in these materials in the nanocrystalline state.

2. Experimental techniques

The FeCuNbSiB sample, in the form of a long thin ribbon of dimensions $l \times w \times t = 200$ mm $\times$ 2 mm $\times$ 0.025 mm, was prepared with a melt–spinning technique at the Vacuumschmelze GmbH, Hanau. The magnetization measurements were performed with an induction technique at room temperature [12]. The magnetizing field $H(t)$ of triangular form with the amplitude $H_0 = 100$ A/m was used for most of the measurements. The exception were the measurements of the dependencie of H_c and remanent magnetization M_r on M_m in which the measurements were performed for different values of H_0. In all measurements, the frequency (f) of the drive field was 5.5 Hz. During the magnetization process, a direct (J_D) or an alternating current $J = J_0 \sin \omega t$, with preselected amplitude, was flowing along the ribbon. J was suitably synchronized with H [7]. For the application of core currents, the sample was supplied with the Pt current leads, spot–welded at the ends of the ribbon. In order to enable the annealing and yet to have the sample in fixed position, the sample was inserted into a thin quartz tube (inner diameter close to the width w of the sample) and fixed into straight position via the Pt current leads.

TABLE 1.

Data relevant to $Fe_{73.5}Cu_1Nb_3Si_{15.5}B_7$ *sample:* T_a *is the annealing temperature;* H_c, M_r, M_m *and* μ_{max} *are the coercive field, remanent magnetization, maximum magnetization and maximum permeability, respectively, determined from the* $M - H$ *loops;* $< \delta >$ *(DC) and* $< \delta >$ *(AC) are the average angles between the magnetization of the domains* (I) *and the ribbon axis deduced from the variations of positions* (C) *of the center of the* $M - H$ *loops and* H_c *with* $H_p(J_D)$ *and* $H_{p0}(J)$, *respectively;* $< S_u >$ *is the average strength of pinning of domain walls. Triangular drive field with the amplitude* $H_0 = 100$ A/m *and frequency* $f = 5.5$ Hz *was used.*

T_a (°C)	H_c (A/m)	$< S_u >$ (A/m)	M_r (T)	M_m (T)	μ_{max} (10^4 Tm/A)	$< \delta >$ (DC)	$< \delta >$ (AC)
prean.	13.5	13.5	0.31	0.49	7.4	3°	4°
200	12.4	12.4	0.29	0.49	6.6	2°	3°
300	8.2	8.2	0.30	0.66	6.5	4°	7°
400	2.5	2.5	0.33	1.26	9.1	1°	1°
450	2.1	2.1	0.23	1.29	9.2	6°	5°
500	2.9	2.9	0.29	1.26	8.2	7°	4°
540	6.5	6.0	0.33	1.21	6.5	24°	22°

The measurements of the $M - H$ loops and $\mathrm{d}M/\mathrm{d}t$ vs. H curves were first performed on as–quenched (amorphous) sample and than repeated after each (successive) annealing step. The annealing temperatures T_a are given in Table 1. The annealing was performed in the flowing argon atmosphere in the long horizontal furnace. The sample was first heated up to T_a (with the average heating rate of about 15 K/min.), kept for one hour at T_a, furnace cooled to 200 °C (average

cooling rate about 3 K/min.) and than removed from the furnace (rapid cooling to room temperature).

In order to get an insight into the microstructure of annealed samples we have annealed a reference sample together with the measured one at $T_a = 450$ °C, 500 °C and 540 °C. The X–ray diffraction pattern of the reference sample (taken after last anneal at 540 °C) has shown peaks corresponding to nanocrystalline phase composed of Fe_3Si grains only. The average diameter D of these grains was calculated by the use of relation $D = 0.9\lambda/(\beta_{1/2}\cos\theta)$, where $\lambda = 1.5418 \times 10^{-10}$ m is the wavelength of the employed X–rays, $\beta_{1/2}$ is the width of the diffraction peak at half of its maximum and θ is the Bragg's diffraction angle. We employed two peaks and obtained very similar values for D ($D = 12$ nm and 14 nm, respectively).

The measurements of the initial AC susceptibility has been used in order to determine the magnetic properties (the Curie temperature T_c) of the as–quenched (amorphous) sample and that annealed at 540 °C. For this purpose, small pieces (≤ 20 mm in length) were cut from the ribbons already used for the measurements of the $M - H$ loops and measured with the standard AC susceptibility technique.

3. *Results and discussion*

The influence of successive annealing on the process of magnetization of FeCuNbSiB sample is illustrated in Fig. 1. Here, the $M - H$ loops and the corresponding $\mathrm{d}M/\mathrm{d}H$ vs. H curves for the as–quenched sample and those after its annealing at $T_a = 450$ °C and 540 °C are shown. We note very different shapes of these curves. From the $M - H$ loops, similar to those depicted in Fig. 1, we have determined the coercive field H_c, the maximum magnetization M_m, the remanent magnetization M_r and the maximum permeability μ_{max} at all annealing temperatures T_a (Table 1). The variations of these parameters with T_a are shown in Figs. 2 and 3. In order to obtain an insight into the changes in the domain structure (which contributes to magnetization for given H_0) and pinning of the corresponding domain walls (DW), we have investigated the effects of the direct (J_D) and alternating (J) core currents (i.e. of the associated surface fields $H_p = J_D/2w$, where w is the width of the ribbon) on the $M - H$ loops after each annealing step. In particular, according to the model for the influence of H_p generated by J_D on the process of magnetization of long and thin amorphous ferromagnetic ribbons, J_D can cause a shift of the $M - H$ loop [4–6]. The position C of the center of the $M - H$ loop is than given by [4–6]:

$$C = \pm H_p \tan < \delta > . \tag{1}$$

Here $< \delta >$ is the average angle between the magnetizations I of the domains contributing to magnetization and the ribbon axis and different signs correspond to different directions of J_D. The same model also predicts that an alternating core current $J = J_0 \sin \omega t$ (suitably synchronized with the magnetizing field H [6])

causes the reduction of H_c [6,7]:

$$H_c = H_{c0} - H_{p0} \tan < \delta >, \tag{2}$$

where H_{c0} is the coercive field in the absence of core current and $H_{p0} = J_0/2w$. Relations (1) and (2) were used in order to deduce $< \delta >$ for different T_a from the variations C and H_c with H_p and H_{p0}, respectively. The knowledge of $< \delta >$ can be used to estimate the average strength of pinning of DWs which contribute to magnetization along the ribbon axis [8,9]:

$$< S_u >= H_{c0} \cos < \delta > . \tag{3}$$

The knowledge of both $< S_u >$ and $< \delta >$ can provide a good insight into the local anisotropy and the MDS, which participates in the process of magnetization for a given amplitude H_0 of the magnetizing field H [8,13].

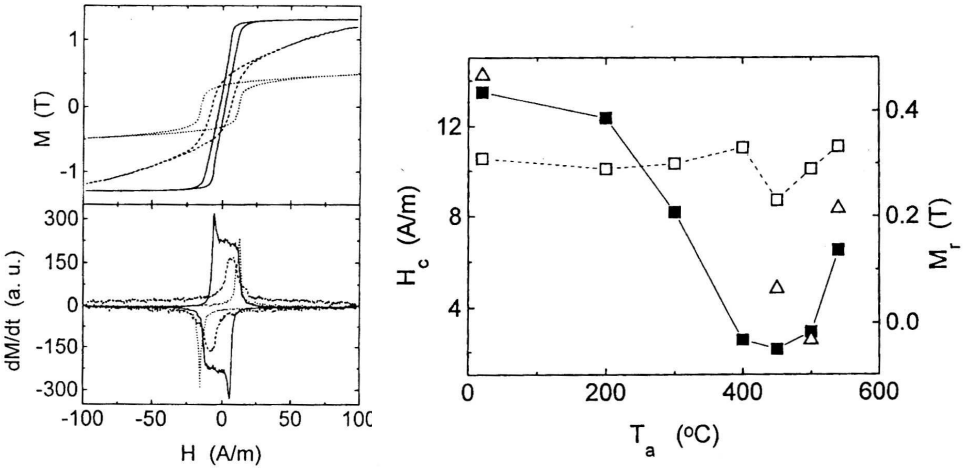


Fig. 1. $M - H$ loops (a) and the corresponding $\mathrm{d}M/\mathrm{d}t$ vs. H curves (b) for $Fe_{73.5}Cu_1Nb_3Si_{15.5}B_7$ sample before annealing (· · · ·) and after annealing at T_a = 450 °C (—) and 540 °C (– – –). The measurements were performed using triangular drive field with the amplitude $H_0 = 100$ A/m and frequency $f = 5.5$ Hz.

Fig. 2. Variation of the coercive field H_c (□) and the remanent magnetization M_r (□) with the annealing temperature T_a for the $Fe_{73.5}Cu_1Nb_3Si_{15.5}B_7$ sample. Symbols △ show the variation of H_c with T_a for the reference sample (see text). The same conditions of measurements as in Fig. 1 were used (right).

From Fig. 1 and the data in Table 1, it is clear that the as–quenched (amorphous) FeCuNbSiB sample has very bad soft magnetic properties (i.e. large H_c = 13.5 A/m and low $M_m \approx 0.35Ms$ for H_0 = 100 A/m). Low M_m and $< \delta > \approx 3°$ (Table 1 and inset in Fig. 3) show that only a fraction of MDS with magnetizations I approximately parallel to ribbon axis participates in the process

of magnetization of amorphous FeCuNbSiB sample for $H_0 = 100$ A/m. Since in the amorphous sample in this range of H_0 the irreversible motion of DWs dominates the magnetization process [2], we conclude that a very strong local anisotropy forms strong volume pinning centres [11] within the sample which for given H_0 prevent the motion of DWs for a sizable fraction ($\approx 50\%$) of MDS. (The existence of a strong local anisotropy in the as–quenched samples was confirmed in the recent investigation of the influence of the torsion and tensile stress on the magnetization of as–quenched FeCuNbSiB samples [10].) Furthermore, the dependence of H_c on M_m/M_s (Fig. 4) shows that a single type of pinning centres determines the motion of DWs responsible for the magnetization of amorphous FeCuNbSiB samples (the slope of $\log H_c$ vs. $\log M_m/M_s$ variation is approximately constant within the explored range of M_m/M_s) [14]. However, M_r tends to saturate for $M_m/M_s > 0.4$ (Fig. 5) in spite of the increase of H_c with M_m/M_s in the same range of M_m (Fig. 4). This seems to indicate that the process of magnetization for $M_m/M_s > 0.4$ involves the bulging of the parts of DWs pinned between the strong pinning centres [14].

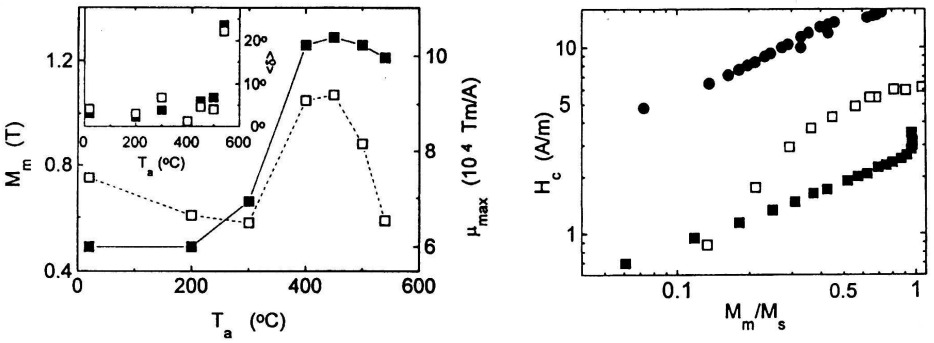


Fig. 3. Variation of maximum magnetization M_m (□) and the maximum permeability μ_{max} (□) with the annealing temperature T_a for the $Fe_{73.5}Cu_1Nb_3Si_{15.5}B_7$ *sample. The conditions of measurements were otherwise the same as in Fig. 1. Inset: the dependence of the average angle $< \delta >$ between the domain magnetizations and the ribbon axis on the annealing temperature T_a for the* $Fe_{73.5}Cu_1Nb_3Si_{15.5}B_7$ *sample. The symbols □ and □ denote $< \delta >$ determined for the direct ($< \delta >$(DC) in Table 1) and alternating core current ($< \delta >$(AC) in Table 1), respectively.*

Fig. 4. Variation of the coercive field H_c with the normalized magnetization M_m/M_s for the $Fe_{73.5}Cu_1Nb_3Si_{15.5}B_7$ *sample in the as–quenched state (○) and after annealing at $T_a = 500$ °C (□) and 540 °C (□). The frequency of the drive field was* 5.5 Hz *(right).*

During the annealing up to $T_a = 300$ °C, H_c decreases quite rapidly with T_a (Fig. 2), whereas M_m increases quite slowly with T_a (Fig. 3). In the same range of T_a, M_r is approximately constant (Fig. 2) and μ_{max} decreases with T_a (Fig. 3). Since the angle $< \delta >$ varies rather little around 4° (inset in Fig. 3) in this range of T_a, it seems that the main reason for decrease of H_c is the reduction of the average pinning strength $< S_u >$ of DWs (Table 1). For $T_a \leq 300$ °C $< S_u >$ most probably

decreases (Table 1) due to the reduction in the local anisotropy associated with the annealing out of the internal stresses and local defects (formed during the sample preparation) [15]. Due to the decrease in the local anisotropy, the same domains from MDS which did not participate earlier in the process of magnetization along the ribbon axis do so after annealing at 300 °C. Their participation is made visible through the simultaneous increase of the angle $< \delta >$ (inset in Fig. 3) and M_m (Fig. 3) at $T_a = 300$ °C. Simultaneously, the participation of domains with different angles δ in the process of magnetization decreases μ_{max}, as observed in Fig. 3 for $T_a \leq 300$ °C.

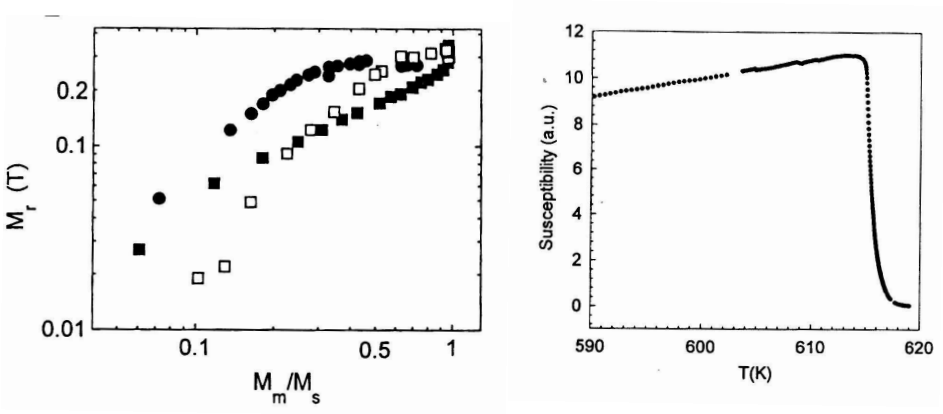


Fig. 5. Variation of the remanent magnetization M_r with the normalized magnetization M_m/M_s for the $Fe_{73.5}Cu_1Nb_3Si_{15.5}B_7$ sample in the as–quenched state (○) and after annealing at $T_a = 500$ °C (□) and 540 °C (□). The frequency of the drive field was 5.5 Hz.

Fig. 6. Variation of the initial susceptibility with the temperature T for the $Fe_{73.5}Cu_1Nb_3Si_{15.5}B_7$ sample in the as–quenched state (right).

After annealing at $T_a = 400$ °C, H_c falls suddenly to 2.5 A/m (Fig. 2 and Table 1), whereas M_m increases to a value close to M_s (Fig. 3). Also μ_{max} suddenly increases at $T_a = 400$ °C (Fig. 3). Figures 2 and 3 show that our sample shows the best soft magnetic properties after annealing at temperatures between 400 °C and 500 °C. In this range of T_a, H_c has the lowest magnitudes (the minimum $H_c \approx 2$ A/m is reached for $T_a = 450$ °C), which means that already the annealing at 400 °C lead to the formation of nanocrystalline Fe_3Si grains [2,3]. The observed variation of H_c with T_a (Fig. 2) is similar to that observed by other authors [2,3], however, due to the prolonged stay of the sample in the furnace (the periods of heating up to T_a and cooling down to 200 °C), the formation of the nanocrystalline phase occurred at somewhat lower temperatures T_a than those reported in the literature [2,3]. In particular, the minimum of H_c is reached at T_a which is some $50 - 90$ °C lower than those observed by the other authors [2,3]. The above conclusion is supported by the measurements for the reference sample which was annealed at $T_a = 450$ °C, 500 °C and 540 °C only. For this sample, H_c reaches minimum at

$T_a = 500$ °C (Fig. 3), i.e. at T_a which is 50 °C higher than that for the sample which spent more time in the furnace. Furthermore, the analysis of the X–ray diffraction patterns for the reference sample (obtained after the anneal at 540 °C) showed the existence of the nanocrystalline grains with the diameters $12 - 14$ nm. The measurements of the Curie temperatures T_c for the amorphous sample and sample annealed at 540 °C also showed the existence of the nanocrystalline phase in the annealed one. As shown in Fig. 6, the amorphous sample exhibits rather sharp transition at $T_c \approx 342$ °C, whereas the sample annealed at 540 °C shows very sharp transition with $T_c \approx 569$ °C (Fig. 7), which corresponds to that of the nanocrystalline Fe–Si grains. Our results for T_c's agree rather well with those of other authors for similar alloys [2,3]. Figure 7 also shows the change in the slope of the initial susceptibility for the annealed sample around 290 °C which probably corresponds to a smeared ferromagnetic transition of the residual amorphous phase. However, since at this stage of annealing the nanocrystalline phase should be the dominant one (about 80% of volume [3]) and the residual (minority) amorphous phase is rather inhomogeneous (concetration fluctuations), its transition (smeared over a sizable temperature range) does not have drastic effect on the susceptibility variation of the annealed sample. Sizably lower average T_c of the residual amorphous phase, compared to that of the as-quenched amorphous sample ($T_c = 342$ °C), is due to change in the composition of amorphous phase after separation of Fe–Si grains (the enrichment in Nb and B and decrease in Fe content).

Upon the formation of the fine structure of Fe_3Si nanocrystalline grains (400 °C $\leq T_a \leq$ 500 °C), the local anisotropy vanishes [2,3], which explains the drastic reduction of H_c and sharp increase of M_m. Very high M_m in this range of T_a (for $T_a = 450$ °C, $M_m \approx M_s$) shows that practically whole domain structure of the sample participates in the process of magnetization. The analysis of the influence of J_D and J on C and H_c (Eqs. (1) and (2)) shows that $< \delta > \approx 4°$ remains quite small (inset in Fig. 3 and Table 1) for 400 °C $\leq T_a \leq$ 500 °C. Rather low $< \delta >$ and large M_m and μ_{max} indicate quite simple domain structure in this range of T_a. The entire domain system seems to consist of domains with magnetizations nearly parallel to the ribbon axis, and the magnetization occurs through the motion of their DWs. The volume pinning of DWs vanishes with the disappearance of the local anisotropy within the sample, and the main DW pinning centres for 400 °C $\leq T_a \leq$ 500 °C are the surface defects and irregularities. The variation of H_c with M_m/M_s for $T_a = 500$ °C, showing two distinctly different regions of the increase of H_c with M_m/M_s (Fig. 4), confirms this conclusion. These two regimes are thought to correspond to two different types of the pinning centres, possesing different strengths [14] (the steeper increase of H_c at elevated M_m corresponds to stronger pinning centres). Therefore, the pinning mechanism of DWs in FeCuNbSiB sample for 400 °C $\leq T_a \leq$ 500 °C is similar to that observed in the nonmagnetostrictive Co–based amorphous ferromagnets [14]. As seen from Fig. 5, for $T_a = 500$ °C, M_r shows the same dependence on M_m/M_s as H_c. This shows that in this range of T_a even the strongest pinning centres are sufficiently weak, which allows that magnetization up to practically M_s occurs via the irreversible motion of DWs.

After the annealing at $T_a = 540$ °C, H_c suddenly increases (Fig. 2 and Table 1). Figure 2 and inset in Fig. 3 show that both $< \delta >$ and $< S_u >$ participate in the increase of H_c. This increase of H_c is most probably associated with the appearance of the uniaxial anisotropy (similar to that induced by torsion in the magnetostrictive amorphous alloys [9,16]), which may arise from the local stresses and/or increased size of the nanocrystalline grains ($D \approx 14$ nm) due to annealing at elevated T_a. The appearance of the anisotropy affects the domain structure [2] and is also confirmed by the rapid decrease of μ_{max}, which starts already for $T_a > 450$ °C (Fig. 3). The shape of the $M - H$ loop for $T_a = 540$ °C (Fig. 1) shows that at lower $H \leq 25$ A/m (i.e. up to $M_m \approx 0.6 M_s$), the magnetization occurs via irreversible motion of DWs, whereas at higher H the reversible rotation processes seem to dominate. The variation of H_c with M_m/M_s for $T_a = 540$ °C (Fig. 4) confirms these conclusions. H_c increases with M_m/M_s to about $M_m/M_s \approx 0.6$ (irreversible motion of DWs), but saturates at larger M_m (reversible rotation processes). M_r shows similar variation with M_m/M_s (Fig. 5) as H_c, which supports the above conclusions about the magnetization processes for $T_a = 540$ °C.

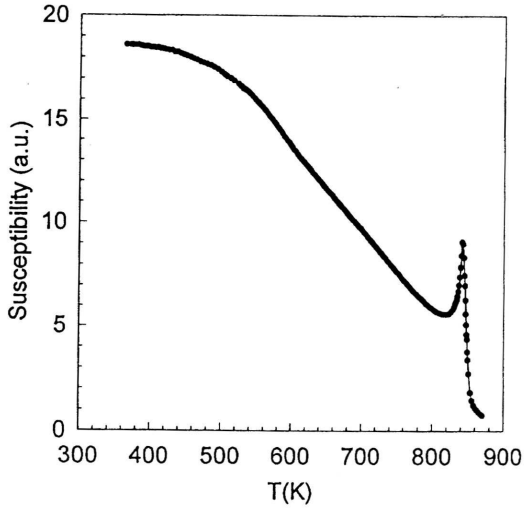


Fig. 7. Variation of the initial susceptibility with the temperature T for the $Fe_{73.5}Cu_1Nb_3Si_{15.5}B_7$ *sample after annealing at* $T_a = 540$ °C.

4. Conclusion

Our results for the changes of the coercive field H_c, remanent magnetization M_r, maximum magnetization M_m and maximum permeability μ_{max} with the annealing temperature T_a for $Fe_{73.5}Cu_1Nb_3Si_{15.5}B_7$ alloy agree well with those obtained for similar FeCuNbSiB alloys [2,3]. The presented analysis of the $M - H$ loops and their changes under the influence of the core currents provides good insight into the domain structure and magnetization processes at different stages of annealing.

Strong volume pinning of domain walls ($< S_u > \approx H_c$), which exist in the sample

in the as–quenched (amorphous) state, decreases initially with T_a ($T_a \leq 300$ °C) due to reduction of the local magnetic anisotropy. This anisotropy vanishes upon the formation of the nanocrystalline structure (400 °C $\leq T_a \leq$ 500 °C), which results in a minimum of $< S_u >$ and H_c and maximum of M_m ($\approx M_s$). In this range of T_a, low $< S_u >$ and angle $< \delta >$, high M_m and Z-shape of the $M-H$ loop show that the entire domain structure is rather simple (the magnetizations of the domains are nearly parallel to the ribbon axis) and the dependence of H_c on M_m/M_s shows that the mechanism of pinning of DWs (surface pinning) is similar to that observed in Co–base nonmagnetostrictive amorphous ferromagnets. Because of this, we conclude that the soft magnetic properties of the nanocrystalline ferromagnetic alloys (especially H_c) can be further improved by eliminating the surface pinning via polishing of the surface, or with some other treatment, which will be studied in our future work.

Acknowledgement

We wish to thank Dr. S. Popović for the X–ray study of the reference sample. Miss. O. Jovanović helped us with the measurements.

References

1) Y. Yoshizawa and K. Yamauchi, IEEE Trans. Magnetics **25** (1989) 3324;
2) B. Hofman, T. Reininger and H. Kronmüller, Phys. Stat. Sol.(a) **134** (1992) 247;
3) G. Herzer, Physica Scripta T **49** (1993) 307;
4) J. Horvat, Phys. Stat. Sol. (a) **129** (1992) 519;
5) S. Sabolek, E. Babić and K Zadro, Fizika A1 (1992) 167;
6) S. Sabolek, IEEE Trans. Magnetics **30** (1994) 919;
7) S. Sabolek, E. Babić and Ž. Marohnić, Phys. Rev. B **48** (1993) 6206;
8) S. Sabolek, E. Babić and M. Šušak, J. Magnetism magnetic Mater. **149** (1995) 331;
9) S. Sabolek, Lj. Erceg and E. Babić, Phys. Stat. Sol. (a) **148** (1995) 283;
10) S. Sabolek, E. Babić and Lj. Erceg, J. Magnetism magnetic Mater., to be published;
11) H. Kronmüller, J. Magnetism magnetic Mater. **24** (1981) 159;
12) J. Horvat, Ž. Marohnić and E. Babić, J. Magnetism magnetic Mater. **82** (1989) 5;
13) P. Schönhuber, H. Pfützner, G. Harasko, T. Klinger and K. Futschik, J. Magnetism magnetic Mater. **112** (1992) 349;
14) J. Horvat, E. Babić, Ž. Marohnić and H. H. Liebermann, J. Magnetism magnetic Mater. **87** (1990) 339;
15) F. E. Luborsky, J. J. Beker and R. O. McCary, IEEE Trans. Magnetics MAG-**11** (1975) 1644;
16) J. M. Barandiaran, A. Hernando and E. Ascasibar, J. Phys. D **12** (1979) 1943;
17) F. Bodker, S. Morup and S. Linderoth, Phys. Rev. Lett **72** (1994) 282.

UTJECAJ UZASTOPNOG NAPUŠTANJA NA PROCESE MAGNETIZIRANJA $Fe_{73.5}Cu_1Nb_3Si_{15.5}B_7$ VRPCE

Model za utjecaj polja H_p, generiranih strujom kroz uzorak, na procese magnetiziranja u feromagnetskim vrpcama iskorišten je za detaljne analize $M - H$ krivulja i odgovarajućih ovisnosti $\mathrm{d}M/\mathrm{d}t$ o H krivuljama uzastopno napuštane $Fe_{73.5}Cu_1Nb_3Si_{15.5}B_7$ vrpce na različitim temperaturama ($T_a \leq 540$ °C). Analize pokazuju da u amorfnom stanju ($T_a \leq 300$ °C) samo dio glavne domenske strukture sudjeluje u procesu magnetiziranja. Napuštanjem na višim temperaturama naglo se smanjuje lokalna anizotropija i srednja jakost zapinjanja domenskih zidova $< Su >$. To rezultira vrlo niskim koercitivnim poljem H_c za 400 °C $\leq T_a \leq$ 500 °C. Istovremeno, maksimalna magnetizacija M_m postaje približno jednaka magnetizaciji saturacije M_s (≈ 1.3 T) u niskom magnetizirajućem polju ($H_0 = 100$ A/m). Minimum H_c ($T_a = 450$ °C) je povezan sa stvaranjem nanokristalnih Fe_3Si zrna, a visoka M_m i maksimalna permeabilnost μ_{max} te mali kut $< \delta >$ (između magnetizacija domena i osi vrpce) pokazuju da je cjelokupna domenska struktura vrlo jednostavna u tom području T_a. Napuštanje na višim temperaturama ($T_a > 500$ °C) izaziva porast $< S_u >$ i $< \delta >$ (zbog čega raste i H_c) te nagli pad μ_{max} što je u skladu s drugim rezultatima za slične uzorke.